Underwater Environment Modeling for Passive Sonar Track-Before-Detect

Daniel Bossér, Robin Forsling, Isaac Skog, Gustaf Hendeby and Magnus Lundberg Nordenvaad

Conference paper

Underwater Environment Modeling for Passive Sonar Track-Before-Detect

Daniel Bossér*, Robin Forsling*, Isaac Skog†‡, Gustaf Hendeby*, Magnus Lundberg Nordenvaad†
* Department of Electrical Engineering, Linköping University, {firstname.lastname}@liu.se
† Swedish Defense Research Agency, {firstname.lastname}@foi.se
‡ Department of Electrical Engineering, Uppsala University, isaac.skog@angstrom.uu.se

***Abstract*—Underwater surveillance using passive sonar and track-before-detect technology requires accurate models of the tracked signal and the background noise. However, in an underwater environment, the signal channel is time-varying and prior knowledge about the spatial distribution of the background noise is unavailable. In this paper, an autoregressive model that captures a time-varying signal level caused by multi-path propagation is presented. In addition, a multi-source model is proposed to describe spatially distributed background noise. The models are used in a Bernoulli filter track-before-detect framework and evaluated using both simulated and sea trial data. The simulations demonstrate clear improvements in terms of target loss and improved ability to discern the target from the noisy background. An evaluation of the track-before-detect algorithm on the sea trial data indicates a performance gain when incorporating the proposed models in underwater surveillance and tracking problems.**

***Index Terms*—Track-before-detect, underwater surveillance, passive sonar, time-varying signal channel, spatially correlated background noise.**

I. Introduction

Underwater surveillance is of critical importance in defense applications and for continuous monitoring of infrastructure against foreign underwater submarines or autonomous vehicles. A recent example is the attack against the Nord Stream pipelines, where experts are emphasizing the need for improved surveillance in the Baltic region. Passive sonar, commonly constructed as an array of hydrophones, is often used for underwater surveillance. The sonar is either towed behind a shaper or placed at a fixed location of strategic interest. By monitoring the underwater environment and potential targets passively, it is less likely that the presence and location of the monitoring system are compromised [1, 2].

While the detection capabilities of the passive systems got better, it is a heads race against the opposing threats making the vehicles quieter [3]. To combat this, the sonar processing technique must be improved to enable detection and tracking at lower signal-to-noise ratio (SNR) conditions. One such technique is the track-before-detect (TkBD) paradigm of detection and tracking. TkBD has seen success in radar tracking applications [4–6], but in the case of sonar in a complex underwater environment several problems remain to be solved before the technology can reach its full potential. It has been shown that TkBD can lower the detection threshold by as much as 6 dB [7, 8]. However, such performance improvements require signal and motion models of high fidelity. Even small model deviations from the true signal and noise statistics might have a large negative impact on the detection and tracking performance.

Fig. 1 shows an example of a bearing-time record (BTR), from a sea trial in the Swedish archipelago where a Saab AUV62 anti-submarine warfare training system was used. The figure shows variations in both the target signal strength and the background noise intensity. TkBD algorithms that incorporate a fluctuating target signal strength have been developed for optical sensors in [9] and radar systems in [10]. These papers demonstrate the importance of considering the target signal strength fluctuations when designing TkBD algorithms. However, in the case of TkBD using passive sonar this aspect has so far not been addressed. In addition, existing TkBD algorithms, e.g., those found in [11, 12], assume that the background noise is both temporally and spatially white. Other approaches circumvent modeling of the background noise through various tricks. For example, [13] compares the beamforming energy within a range of bearings close to the target estimate to energies in neighboring bearings. Another approach, presented in [14], averages the observed beamforming energies over the history of confirmed or tentative track bearings. In this case, the underlying idea is that the received signal energy from the target on average is higher than any clutter or noise in the background. Common for these methods is that when applied to a tracking scenario as illustrated in Fig. 1, they either fail to detect and track the target or generate many false tracks. The false detections are caused by the methods' inability to distinguish the spatially correlated background noise from potential targets. Furthermore, the SNR of the target signal varies quickly, and the source signal intermittently becomes indistinguishable from the background noise, which provides an additional challenge. Therefore, in this paper, two models describing

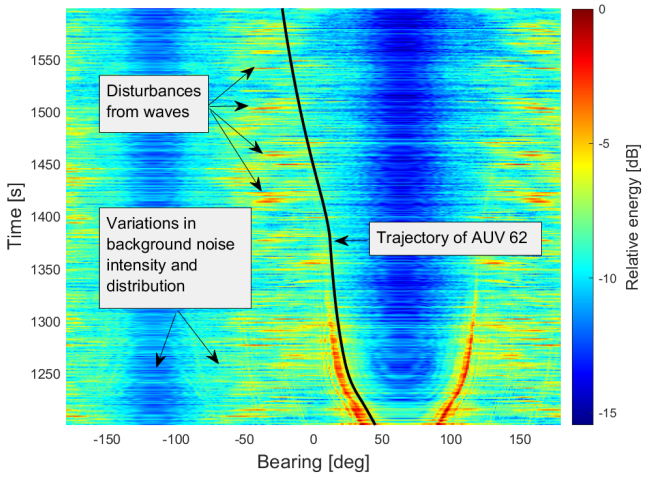

Fig. 1. BTR from a passive sonar system. The black line shows the bearing of an AUV passing by the sonar system. Two phenomena that make it difficult to detect and track the AUV are apparent in the figure. There are large variations in the background noise intensity at different bearings, and the received signal energy from the AUV varies rapidly.

- the variations in the received source signal level, and
- the spatial correlations in the background noise,

are presented. The models are integrated into a TkBD framework and evaluated using both simulated and sea trial data.

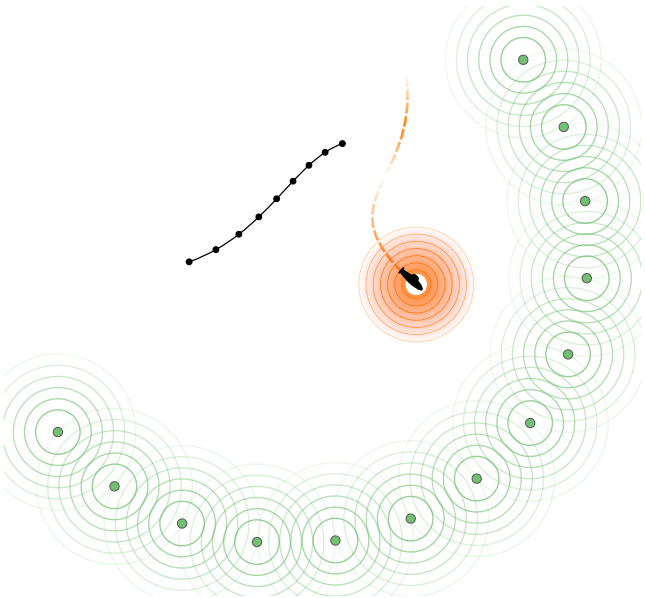

Fig. 2. Simplified illustration of the considered target tracking scenario, where the problem is to detect and track a potential target moving in the proximity of a hydrophone array in a noisy environment. The spatially correlated noise is modeled as a sum of point sources at different bearings.

II. Track-Before-Detect Using Passive Sonar

Consider a single target Bernoulli filter TKBD algorithm like that presented in [11]. Two key components of the TkBD algorithm are the state evaluation Markov model and the measurement likelihood function. The Markov model $\phi(X_k|X_{k-1})$ describes the time dynamics of a state X_k, while the likelihood function $\varphi(z_k|X_k)$ describes the probability of receiving measurements z_k given a certain state X_k.

A. Single-Target State Estimation Filter

At any time k the target is either present or absent. If the target is present, then its state at time k is x_k. This is incorporated into the TkBD algorithm using a random finite set (RFS) framework [15]. In particular, the probability density function (PDF) of the target RFS X_k is modeled as a Bernoulli RFS

$$p(X_k) = \begin{cases} 1 - q_k, & \text{if } X_k = \varnothing, \\ q_k s(x_k), & \text{if } X_k = \{x_k\}, \end{cases} \tag{1}$$

where q_k is the target existence probability and $s(x_k)$ is the PDF of x_k, all at timestep k. The posterior distribution of X_k given all the measurements up to time k can be recursively calculated using

$$p(X_k|z_{1:k}) = \frac{\varphi(z_k|X_k)p(X_k|X_{k-1})}{\int \varphi(z_k|X_k)p(X_k|z_{1:k-1})\,\delta X_k}, \tag{2a}$$

$$p(X_{k+1}|z_{1:k}) = \int \phi(X_{k+1}|X_k)p(X_k|z_{1:k})\,\delta X_k, \tag{2b}$$

where $p(X_k|z_{1:k})$ and $p(X_{k+1}|z_{1:k})$ are the posterior and predicted PDFs, respectively, and

$$z_{1:k} \triangleq \{z_1, z_2, \ldots, z_k\} \tag{3}$$

are all the measurements leading up to time step k. To implement the recursions, accurate specification of the Markov model and likelihood function is required, as the accuracy of the calculated posterior distribution will depend directly on them.

B. Likelihood Function

Consider a scenario where a single M-element array is used to detect and track the bearing ψ_k of the target. The N sound samples recorded during time slot k by the m:th hydrophone is in [11] modeled as

$$y_{k,m} = W^* \Lambda_m(\psi_k) W v_k + e_{k,m}. \tag{4}$$

Here, W is the unitary discrete Fourier transform matrix, v_k is signal emitted from the target, and $e_{k,m}$ is noise. Moreover, $\Lambda_m(\psi_k)$ describes the phase shift of the signal v_k in hydrophone m due to the propagation delay of the signal as it arrives from angle ψ_k. If the target sound and measurement noise are assumed to be normally distributed as $v_k \sim \mathcal{N}(0, \sigma_{v_k}^2 I_N)$ and $e_{k,m} \sim \mathcal{N}(0, \sigma_e^2 I_N)$, then the likelihood for the observation

$$z_k = \begin{bmatrix} y_{k,1}^\mathsf{T} & \ldots & y_{k,m}^\mathsf{T} \end{bmatrix}^\mathsf{T}, \tag{5}$$

becomes

$$\varphi(z_k|X_k) = \begin{cases} \mathcal{N}(z_k; 0, R_1), & \text{if } X_k = \varnothing, \\ \mathcal{N}(z_k; 0, R_2(x_k)), & \text{if } X_k = \{x_k\}. \end{cases} \tag{6}$$

Here, the covariance matrices are

$$R_1 = I_{NM}\sigma_e^2, \tag{7a}$$

$$R_2(x_k) = (I_M \otimes W^*)(I_{NM}\sigma_e^2 + \sigma_{v_k}^2 U^*(\psi_k)U(\psi_k)) \times (I_M \otimes W), \tag{7b}$$

where

$$U(\psi_k) = \begin{bmatrix} \Lambda_1^*(\psi_k) & \ldots & \Lambda_M^*(\psi_k) \end{bmatrix}. \tag{8}$$

Note that $R_2(x_k)$ depends on $\sigma_{v_k}^2$, which must be estimated.

C. Markov Model

The Markov model for x_k is considered here. For additional details about the Markov model for the RFS state X_k, which includes the target existence probability q_k, the reader is referred to [15]. Let ψ_k and $\omega_k = \dot{\psi}_k$ denote the bearing and bearing rate of the target at time k, respectively. Moreover, let

$$\eta_k = 10 \log_{10}\left(\frac{\sigma_{v_k}^2}{\sigma_e^2}\right), \tag{9}$$

be the SNR at time k. Next, define the target state as

$$x_k = \begin{bmatrix} \psi_k & \omega_k & \eta_{k:k-L} \end{bmatrix}^\mathsf{T}, \tag{10}$$

where $\eta_{k:k-L} = \begin{bmatrix} \eta_k & \eta_{k-1} & \ldots & \eta_{k-L} \end{bmatrix}$ and $L \geq 0$. The Markov model is then given by

$$\phi(x_{k+1}|x_k) = \mathcal{N}(x_{k+1}; F_k x_k, Q_k), \tag{11}$$

where

$$F_k = \begin{bmatrix} F_k^{(1)} & 0 \\ 0 & F_k^{(2)} \end{bmatrix}, \qquad Q_k = \begin{bmatrix} Q_k^{(1)} & 0 \\ 0 & Q_k^{(2)} \end{bmatrix}. \tag{12}$$

The matrices $F_k^{(1)}$ and $Q_k^{(1)}$ correspond to a constant velocity model for the bearing. The dynamics of η_k are described by $F_k^{(2)}$ and $Q_k^{(2)}$, which will be discussed next. In the baseline algorithm [11] $L = 0$, $F_k^{(2)} = 1$, $Q_k^{(2)} = \sigma_{\eta_k}^2$ and hence the SNR is modeled as a random walk

$$\eta_{k+1} = \eta_k + \varepsilon_k, \tag{13}$$

where $\varepsilon_k \sim \mathcal{N}(0, \sigma_{\eta_k}^2)$.

III. Modeling A Time-Varying Signal-To-Noise Ratio

If the received source signal energy fluctuates rapidly, the random walk model for the SNR used in [11] will typically result in poor target tracking capabilities. Assuming the fluctuations to be somewhat periodical, a better model for the SNR may be an autoregressive (AR) model. In that case $F_k^{(2)}$ and $Q_k^{(2)}$ are given by

$$F_k^{(2)} = \begin{bmatrix} \beta_k & 0 & 0 \\ I_L & & 0 \end{bmatrix}, \qquad Q_k^{(2)} = \mathrm{diag}(\sigma_{\eta_k}^2, 0, \ldots, 0). \tag{14}$$

Here $\beta_k = \begin{bmatrix} \beta_{1,k} & \ldots & \beta_{p,k} \end{bmatrix}$ and $\sigma_{\eta_k}^2$ denote the AR parameters and process noise variance, respectively, and p is the AR model order.

The AR parameters and process noise are typically unknown and time-varying. However, assuming them to be slowly varying they may be estimated from historical data in an outer-loop separated from the TkBD algorithm. Here it is suggested that the AR parameters in β_k are estimated using a sliding window approach. Assume that $\eta_{k:k-L}$ is available, where L determines the length of the sliding window. From this it is possible to use the Yule-Walker equations where the AR model is used to construct a linear system of equations that relates β_k and $\eta_{k:k-L}$ [16]. An estimate $\hat{\beta}_k$ of β_k is then computed using the least squares method. Note, L must be chosen large enough for the considered linear system of equations to be solvable.

IV. Spatial Correlation Modeling Through Point Sources

From Fig. 1 it is clear that the background noise is not spatially white as assumed in the likelihood presented in (4). This will cause the TkBD algorithm to produce frequent false detections as it cannot distinguish between true signal sources and spatially distributed noise sources. To overcome this problem a noise model consisting of a sum of point noise sources located in the far field is proposed. See Fig. 2 for a conceptual illustration of the proposed noise model.

Recall that $y_{m,k}$ is the signal observed in hydrophone m, and that (4) provides a model of $y_{m,k}$ given that there is one sound source located at bearing ψ_k. In the case that there are several spatially distributed sources of noise present, a natural extension to the model is

$$y_{k,m} = W^* \Lambda_m(\psi_k) W v_k + \sum_{l=1}^{L} W^* \Lambda_m(\psi^l) W \epsilon_{l,k} + e_{k,m}. \tag{15}$$

Here, ψ^l is the bearing to noise source l from which the noise signal $\epsilon_{l,k}$ originates. Moreover, it is assumed that the noise signal from each of the sources are mutually independent and distributed as $\epsilon_{l,k} \sim \mathcal{N}(0, \sigma_l^2 I_N)$.

With the additional noise terms, the covariance matrix of z_k becomes

$$R_i(x_k) = (I_M \otimes W^*)\, B_i(\psi_k)\, (I_M \otimes W), \quad i = 1, 2, \tag{16}$$

where

$$\begin{aligned} B_i(\psi_k) = {} & \sigma_v^2 U(\psi_k) U(\psi_k)^* \delta(i-2) \\ & + \sum_{l=1}^{L} \sigma_l^2 U(\psi^l) U(\psi^l)^* + I_{NM} \sigma_e^2. \end{aligned} \tag{17}$$

The proposed likelihood function is then given by replacing R_i in (6) with (16).

Table I
Description of the models used

Name	Description
Benchmark	The method used in [11]. Assumes that the noise is temporally and spatially white and that the source signal strength varies slowly.
SN-RW	*Spatial noise random walk SNR*. Assumes the noise to be spatially correlated and the source signal strength to vary slowly.
SN-AR	*Spatial noise AR SNR dynamics*. Assumes the noise to be spatially correlated and the source signal strength to fluctuate rapidly.

A. Estimation of Source Strength

To use the likelihood in (6) with the spatial noise covariance matrix in (16) one must first have a description of the spatial noise. If the bearings $\{\psi_l\}_{l=1}^{L}$ are known, the parameters $\theta = \{\sigma_e^2, \sigma_1^2, \ldots \sigma_L^2\}$ must be specified. These parameters can be estimated using a sequence of data where no target is present. Let $R_1(\theta)$ be a parametrization of R_1 in terms of the unknown parameters θ. Given a set of measurements $z_{1:K}$ where it is known that there is no target contribution to the signal, θ can be estimated as

$$\hat{\theta} = \arg\min_{\theta} \left\| R_1(\theta) - \frac{1}{K} \sum_{k=1}^{K} z_k z_k^T \right\|_F^2. \tag{18}$$

Additionally, let $\hat{\theta}(z_k)$ denote the estimate given a single measurement z_k in (18).

V. Evaluation

To better understand the impact of both the spatial noise model and the SNR variation model, combinations of the two models are evaluated on a simulated and a real-world dataset and compared to the suggested method in [11]. These combinations are listed in Table I. Of extra interest is the tendency of the trackers to confuse the noisy environment for a target and the loss of tracks as the SNR temporarily becomes worse. These challenges are present in the real-world dataset and hence are also introduced in the simulations.

To summarize, it is shown on the simulated dataset that including information about the spatial noise improves the tracker's robustness against false alarms. Moreover, usage of the SNR variation model results in less drastic drops in the estimated target existence probability $\hat{q}_k$. The results on the real-world dataset show indications of similar nature.

A. Spatial Source Strength Estimation

Fig. 3a shows a BTR for a sequence of 750 timesteps (187 s) where the target was not present. The bearings of the $L = 180$ spatial sources used to model the spatially correlated noise cover the half circle in front of the array, i.e., one source for every degree. An estimate of the spatial source strength, given that a source is placed at every bearing ψ and the sequence of measurements $z_1, \ldots, z_{750}$ is shown in Fig. 3b. Additionally, the single measurement estimates $\hat{\theta}(z_k)$ are shown as a gray histogram in the same figure, together with its 90 % percentile denoted by $\hat{\theta}_{90}$.

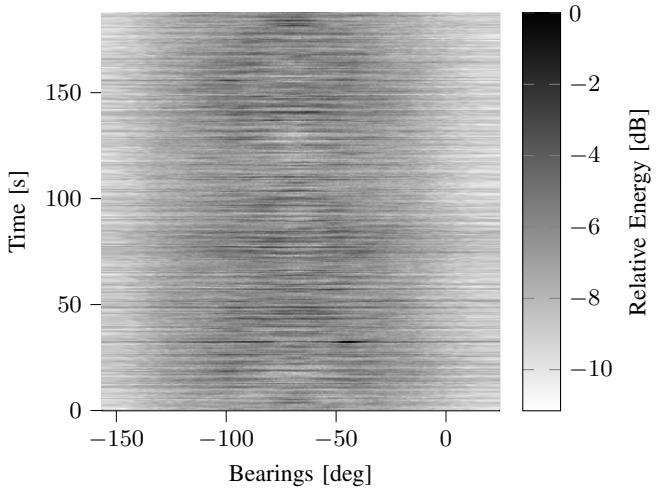

(a) BTR of the data segment that is used to estimate the noise model parameters.

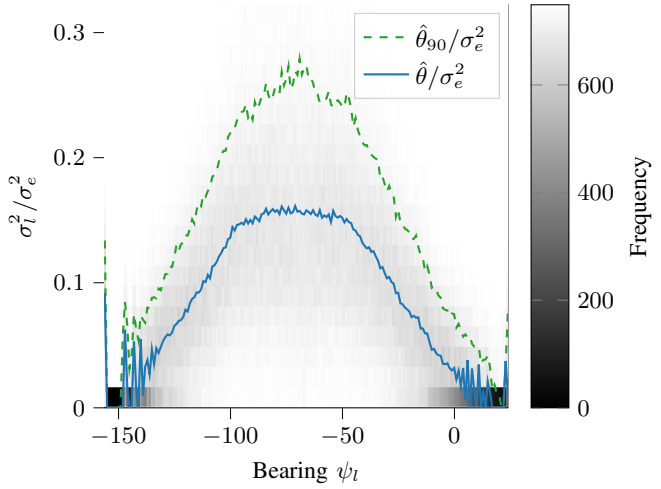

(b) Estimated variances of the signals emitted by the spatial sources. The histogram shows the estimated variance $\hat{\theta}(z_k)$ for each of the 750 batches. The blue solid line shows the estimated variance $\hat{\theta}$ with respect to all batches, as in (18). Finally, the green dashed line shows the 90 % quantile with respect to the $\hat{\theta}(z_k)$ estimates.

Fig. 3. The estimated spatial noise model and its dataset.

B. Simulation

The methods are tested in a target tracking case that mimics the data seen in Fig. 1. That is, the hydrophone array used in the simulation uses the same relative positions as in the real dataset. Moreover, the spatial noise source powers θ used in the simulation are estimated from the real dataset, that is $\hat{\theta}$ from (18) shown in Fig. 3b.

The bearing of the target changes according to a constant velocity model, and the ground truth SNR η changes as

$$\eta_k = 10 \log_{10} \sin^2(\omega_0 T k) - 5\,[dB], \tag{19}$$

where $T = 0.25\,\text{s}$ and $\omega_0 = 2\pi \cdot 0.2\,\text{rad/s}$. This corresponds to a signal that is amplitude-modulated with a sinusoid function. To rigorously test the trackers, the simulated dataset starts with a sequence of 80 steps (20 s) without a target. The target is then introduced and is present for 20 s, followed by another 80 steps without a target. This generates the BTR as seen in Fig. 4a. The estimated bearings $\hat{\psi}_k$ for which $\hat{q}_k > 0.9$ according to the different methods for a single run can be seen in Fig. 4b. Finally, the average $\hat{q}_k$ of 100 Monte Carlo (MC) runs is shown in Fig. 4c.

It can be seen in Fig. 4b that the benchmark filter occasionally confuses spatial noise for the target, resulting in a bearing estimate that is very different from the ground truth. By including a description of the spatial noise properties, as has been done in the SN-RW filter, this is no longer seen. However, the filter still loses the track as the SNR momentarily drops. The detection probability for the duration of the target's existence is also improved after inclusion of the spatial noise model, as seen in Fig. 4c.

The SN-AR filter is less susceptible to target loss, but it comes at the cost of more time steps before it realizes that the target is absent. This is also reflected in the mean $\hat{q}_k$ in Fig. 4c, showing a low-pass-filter-like effect on $\hat{q}_k$, which also explains the improvement to the track loss. For the duration of the target presence, the SN-AR filter outputs the highest estimated probability of existence.

C. At Sea Trial

The methods were also evaluated using a real-world dataset. The dataset was collected in the Stockholm archipelago, where a 55-element hydrophone array sampled data while a Saab AU64 submarine warfare training system moved in the proximity of the array, acting as the target. The hydrophone positions were estimated using signals of opportunity and SLAM as described in [17].

Since there is a target present during the whole examined sequence, the filters are compared to human performance. Experts at the Swedish Defence Research Agency (FOI) were asked to indicate the presence and bearing of a target in a set of shuffled BTR sequences, each of 36 s length.

All filters used the same spatial noise power model, with the power estimates $\hat{\theta}_{90}$, except for the benchmark filter. Using a spatial noise model that assumes more power in each of the spatial noise sources, compared to $\hat{\theta}$, makes the filters more robust against temporary changes in the background noise.

The results from the evaluation with the sea trial dataset bear similarities with the results from the simulation, see Fig. 5b. The benchmark filter tends to mistake spatial noise source variations for a target. The filter is also approximately 10 s slower at initiating the tracking, compared to its spatial noise-aware counterparts. Compared between SN-RW and SN-AR, the SN-AR filter estimates a track as a continuous track, while the SN-RW filter occasionally loose-track of the target. SN-AR filter is also seemingly able to follow the target for a longer duration, closer to the track that the experts labeled. There is a tendency among the filters to output the extreme values, that is, either $\hat{q}_k = 0$ or $\hat{q}_k = 1$, as seen in Fig. 5c. The benchmark filter shows a more erratic estimate, something that is also observed in the SN-RW filter but to a lesser extent. The SN-AR filter shows a smoother output, with a slower drop in estimated existence probability compared to other methods.

VI. Conclusions and Future Work

To summarize, this paper presented a multi-source noise model to describe the spatially correlated background noise and an adaptive

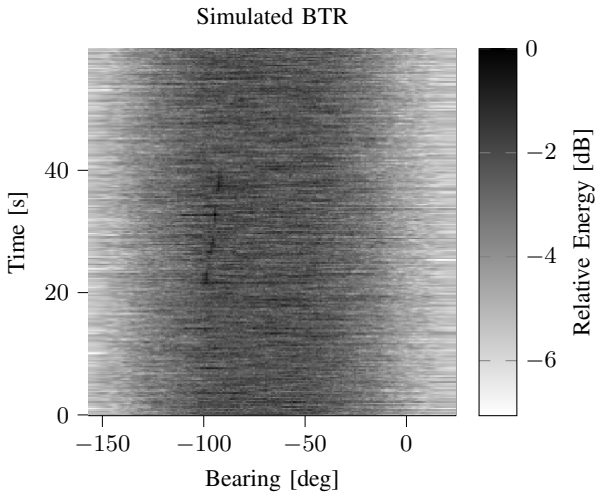

(a) BTR of the generated dataset. The target appears after 20 s and disappears after an additional 20 s. The SNR of the target fluctuates with a frequency of 0.2 Hz with a peak amplitude at -5 dB.

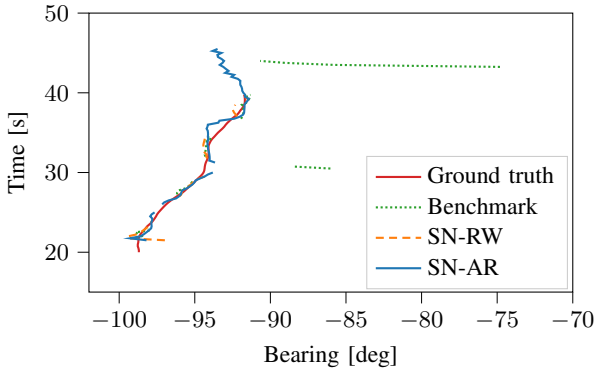

(b) Ground truth bearing and the estimated trajectory according to the examined filters. The estimated bearing $\psi_{k|k}$ is only drawn if $q_{k|k} > 0.9$.

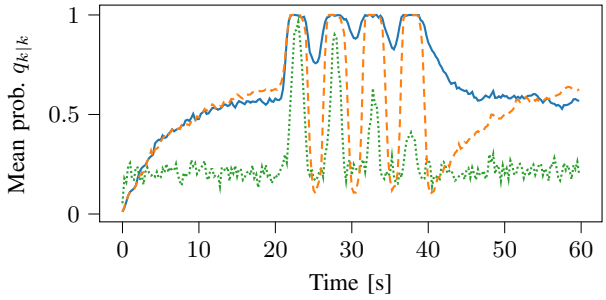

(c) Estimated probability of existence $q_{k|k}$ by the filters.

Fig. 4. Simulated dataset and results.

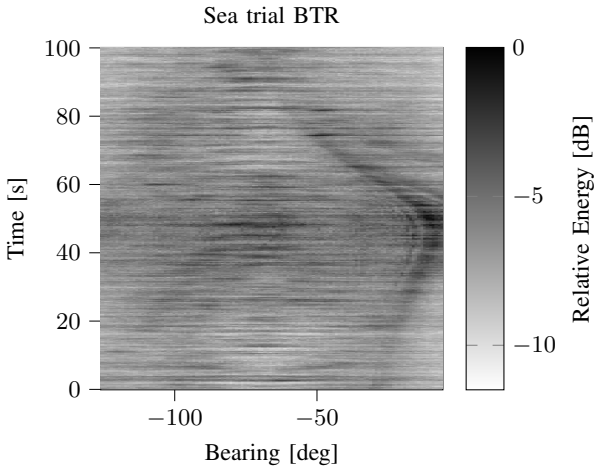

(a) BTR of a part of the real dataset.

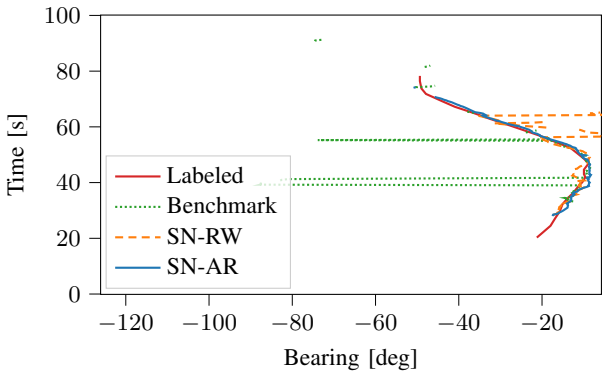

(b) Estimated bearings $\psi_{k|k}$ for which the filters have output $q_{k|k} > 0.9$. The red line shows the estimated target track according to the survey conducted at FOI.

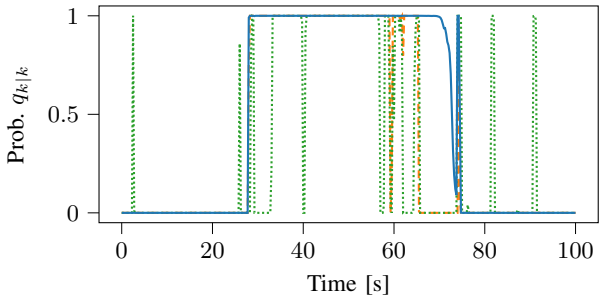

(c) Estimated probability of existence by the filters given the BTR sequence in Fig. 5a.

Fig. 5. Real-world dataset and results.

autoregressive model to handle the SNR fluctuations originating from the changes in the underwater channel. This was integrated into a TkBD algorithm, and was evaluated with a simulated and a real-world dataset. It has been shown, on the simulated dataset, that the multi-source model lessens the probability that the filter mistakes the background noise for the target, and that the inclusion of the autoregressive SNR model improves the filter in terms of track loss. Similar results have been observed on the real-world dataset.

Some challenges remain to be solved. While the spatial correlations in the background noise are accounted for in the current measurement model, the temporal ones remain. The background noise is not static in its nature, explained by short-term phenomena such as breaking waves on the surface. Hence, future research may focus on modeling this process by considering two classes of targets, one of which is the moving target, the other of which is a temporary stationary target with a short life span. This may be done by utilizing an RFS framework for modeling multiple targets. Additionally, the filters have been observed to be overly confident in the spatial noise model, hence the need to use the estimates $\hat{\theta}_{90}$. A Bayesian modeling approach, where θ is instead assumed to be random and is estimated a posteriori, may solve this issue.

REFERENCES

[1] H. Selhammer, "Passive acoustic bearing estimation algorithms applied on hydro acoustic data," FOI – Swedish Defence Research Agency, Stockholm, Sweden, Tech. Rep. FOI-R – 1923 – SE, Feb. 2006.

[2] C. Kopp, "Identification underwater with towed array sonar," *Defense Today*, pp. 32–33, Dec. 2009.

[3] O. R. Cote Jr., "Invisible nuclear-armed submarines, or transparent oceans? Are ballistic missile submarines still the best deterrent for the united states?" *Bulletin of the Atomic Scientists*, vol. 75, no. 1, pp. 30–35, Jan. 2019.

[4] F. Papi, V. Kyovtorov, R. Guiliani, F. Oliveri, and D. Tarchi, "Bernoulli filter for track-before-detect using MIMO radar," *IEEE Signal Processing Letters*, vol. 21, no. 9, pp. 1145–1149, Sep. 2014.

[5] B. Errasti-Alcala, W. Fuscaldo, P. Braca, and G. Vivone, "Realistic extended target model for track before detect in maritime surveillance," in *Proceedings of the 2015 IEEE OCEANS*, Genova, Italy, May 2015, pp. 1–9.

[6] F. Santi, D. Pastina, and M. Bucciarelli, "Experimental demonstration of ship target detection in GNSS-based passive radar combining target motion compensation and track-before-detect strategies," *Sensors*, vol. 20, no. 3, Jan. 2020.

[7] M. Mallic, V. Krishnamurthy, and B. Vo, *Integrated Tracking, Classification, and Sensor Management: Theory and Applications*. Wiley-IEEE Press, 2012, ch. 8, pp. 315–318.

[8] W. Li, W. Yi, M. Wen, and D. Orlando, "Multi-PRF and multi-frame track-before-detect algorithm in multiple PRF radar system," *Signal Processing*, vol. 174, Sep. 2020.

[9] S. Tonissen and Y. Bar-Shalom, "Maximum likelihood track-before-detect with fluctuating target amplitude," *IEEE Transactions on Aerospace and Electronic Systems*, vol. 34, pp. 796–809, Jul. 1998.

[10] M. G. Rutten, N. J. Gordon, and S. Maskell, "Recursive track-before-detect with target amplitude fluctuations," *IEE Proceedings - Radar, Sonar and Navigation*, vol. 152, pp. 345–352, Oct. 2005.

[11] D. Bossér, G. Hendeby, M. L. Nordenvaad, and I. Skog, "A statistically motivated likelihood for track-before-detect," in *Proceedings of the IEEE International Conference on Multisensor Fusion and Integration*, Cranfield, UK, Sep. 2022, pp. 1–6.

[12] L. Xu, C. Liu, W. Yi, G. Li, and L. Kong, "A particle filter track-before-detect procedure for towed passive array sonar system," in *Proceedings of the 2017 IEEE Radar Conference*, Seattle, WA, USA, Jun. 2017, pp. 1460–1465.

[13] A. Gunes and M. B. Guldogan, "Joint underwater target detection and tracking with the Bernoulli filter using an acoustic vector sensor," *Digital Signal Processing*, vol. 48, pp. 246–258, Jan. 2016.

[14] T. Northardt and S. C. Nardone, "Track-before-detect bearings-only localization performance in complex passive sonar scenarios: A case study," *IEEE Journal of Oceanic Engineering*, vol. 44, pp. 482–491, Apr. 2019.

[15] B. Ristic, B.-T. Vo, B.-N. Vo, and A. Farina, "A tutorial on Bernoulli filters: Theory, implementation and applications," *IEEE Transactions on Signal Processing*, vol. 61, no. 13, pp. 3406–3430, 2013.

[16] A. V. Oppenheim and R. W. Schafer, *Discrete-Time Signal Processing*, 3rd ed. Upper Saddle River, NJ, USA: Prentice Hall, 2009.

[17] I. Skog and E. Gudmundson, "Signals of opportunity based geometry calibration of hydrophone arrays," in *Proceedings of the 2019 IEEE OCEANS*, Seattle, WA, USA, Oct. 2019, pp. 1–5.